

Super-resolution using Barker-based array projected via spatial light modulator

Asaf Ilovitsh,^{1,*} Tali Ilovitsh,¹ Eyal Preter,¹ Nadav Levanon,² and Zeev Zalevsky¹

¹Faculty of Engineering, Bar-Ilan University, Ramat-Gan 5290002, Israel

²School of Electrical Engineering, Faculty of Engineering, Tel-Aviv University, Tel-Aviv 6997801, Israel

*Corresponding author: ilovitsh@gmail.com

Received February 20, 2015; accepted March 24, 2015;
posted March 25, 2015 (Doc. ID 235051); published April 10, 2015

The use of a two-dimensional Barker-based array in the conventional time multiplexing super-resolution (TMSR) technique was recently presented [Opt. Lett. **40**, 163–165 (2015)]. It enables achieving a two-dimensional SR image using only a one-dimensional scan, by exploiting its unique auto-correlation property. In this Letter, we refine the method using a mismatched array for the decoding process. The cross-correlation between the Barker-based array and the mismatched array has a perfect peak-to-sidelobes ratio, making it ideal for the SR process. Also, we propose the projection of this array onto the object using a phase-only spatial light modulator. Projecting the array eliminates the need for printing it, mechanically shifting it, and having a direct contact with the object, which is not feasible in many imaging applications. 13 phase masks, which generate shifted Barker-based arrays, were designed using a revised Gerchberg–Saxton algorithm. A sequence of 13 low resolution images were captured using these phase masks, and were decoded using the mismatched arrays, resulting in a high-resolution image. The proposed mismatched array and the design process of the phase masks are presented, and the method is validated by a laboratory experiment. © 2015 Optical Society of America

OCIS codes: (100.6640) Superresolution; (100.0100) Image processing; (100.5090) Phase-only filters; (070.6120) Spatial light modulators.

<http://dx.doi.org/10.1364/OL.40.001802>

A perfect imaging lens with a finite aperture is diffraction limited. This dictates a restriction on the minimal distance at which two point sources can be resolved using this lens. The minimal distance was defined by Abbe to be proportional to the optical wavelength, and to the F number of the imaging system [1]. One of the most common methods of super-resolution (SR) which overcomes the diffraction limitation is time multiplexing super-resolution (TMSR), originally suggested by Françon [2]. These techniques improve the spatial resolution at the expense of the time domain using some *a priori* knowledge on the inspected object. The main concept was proposed by Lukosz [3], and includes the use of two moving gratings that are shifted between time frames during the imaging sequence. The first grating is placed near the object and encodes the spatial information, and the second grating is placed near the image and decodes the spatial information. The second grating may be added digitally via computer means [4].

In a previous paper, we proposed the use of a binary transmission Barker-based array as the encoding and decoding mask in the conventional TMSR method [5]. This array is a two-dimensional (2D) generalization of the one-dimensional (1D) Barker code [6], which is commonly used in radar signals [7]. The Barker-based array has several advantages over previous methods. This array has a unique 2D auto-correlation (AC) property which enables it to generate a 2D SR image with a 1D scanning of the object, regardless of the scanning direction. Furthermore, since the Barker-based array has a constant AC sidelobes value, it requires significantly smaller number of images than the number required in the random noise method [8].

A Barker code is a N length sequence of digits, where each bit has a value of -1 or 1 . The Barker code has an ideal a-periodic AC property, such that the peak

magnitude of the AC equals N , and the sidelobes magnitudes are 0 or 1. The Barker codes also have a two-valued cyclic (periodic) AC. This means that the sidelobes AC value of a cyclic Barker code has a constant value. In optical amplitude masks, the value -1 is not valid, since there cannot be a negative number in an amplitude mask. Thus, each -1 in the Barker code is replaced by 0. This modified Barker sequence maintains its two-valued cyclic AC property.

Since a true 2D unipolar Barker array does not exist for arrays larger than 2×2 [9,10], a generalization of the Barker code into a 2D array was performed as follows: the first row in the array is a standard 1D Barker code, and each row in the array is shifted with respect to the previous row.

The longest reported Barker code is 13 bits long [11]. Using its unipolar representation [1111100110101], a 13×13 array was established. Each row in the array is shifted 5 pixels to the right in respect to the previous row. This 2D array, which will be the encoding mask, is presented in Fig. 1(a).

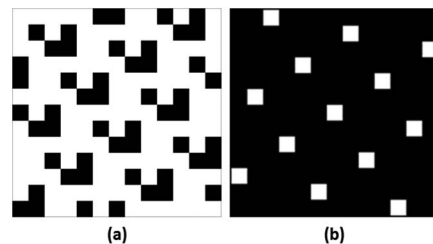


Fig. 1. (a) A 13×13 Barker-based array, where each row is a 5 pixels shift of the previous row. (b) The cyclic CC of the 13×13 Barker-based array with the mismatched array. Pixels values: white, 1; black, 0.

For the decoding mask, a mismatched filter is used. Since the process is in 2D, the mismatched filter is also an array. The mismatched array is based on the same Barker-based array, with the following change: each pixel of 0 in the array is transformed into -2 . For example, the first row in the mismatched array is [11111-2-211-21-21]. Since the decoding mask is added digitally, negative values are allowed. The cyclic cross-correlation (CC) of the Barker-based array with the mismatched array has a perfect peak to sidelobes ratio. Namely, it has N peaks equal to 1, and sidelobes between the peaks that equal 0. The distance between each two peaks is $\sqrt{13}$. The CC is presented in Fig. 1(b).

Following the conventional TMSR 4f system (presented in Fig. 2), the blurred output intensity, before the second mask, is given by

$$I_{\text{img}}(x, y, t) = \int_{-\infty}^{\infty} \int_{-\infty}^{\infty} I_{\text{obj}}(x', y') \cdot M_1(x' - vt, y') p(x - x', y - y') dx' dy', \quad (1)$$

where I_{obj} is the object intensity, M_1 is the encoding mask, v is its velocity, and p is the point spread function (PSF).

The decoding process involves the multiplication of each image with the appropriate decoding mask M_2 , and their integration over time:

$$R(x, y) = \int_{-\infty}^{\infty} I_{\text{img}}(x, y, t) M_2(x - vt, y) dt. \quad (2)$$

The encoding and decoding masks are the only time-dependent variables. Thus, changing the integrals' order is allowed. Assuming M_1 is the Barker-based array, and M_2 is the mismatched array, the time integral becomes

$$\int_{-\infty}^{\infty} M_1(x - vt, y) M_2(x' - vt, y') dt = \sum \delta(x - x', y - y'). \quad (3)$$

The result is a set of Dirac deltas [as presented in the 13 bits example in Fig. 1(b)]. Introducing the time integral into Eq. (2) yields

$$R(x, y) = \int_{-\infty}^{\infty} \int_{-\infty}^{\infty} I_{\text{obj}}(x', y') p(x - x', y - y') \cdot \left[\sum \delta(x - x', y - y') \right] dx' dy'. \quad (4)$$

Assuming the PSF is smaller than the distance between two peaks, the integral becomes

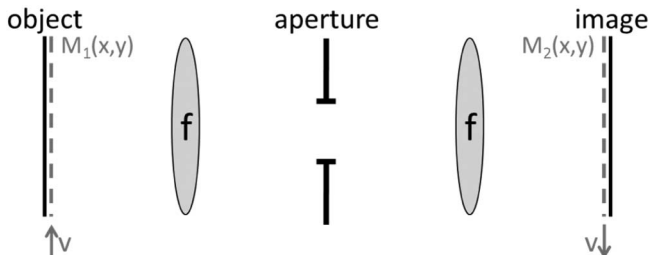


Fig. 2. Conventional TMSR 4f system.

$$R(x, y) = p(0, 0) I_{\text{obj}}(x, y), \quad (5)$$

which means that the reconstruction is exactly the high-resolution (HR) image, up to a constant.

In the previous paper, the Barker-based array was printed, placed on top of the object, and mechanically shifted. That approach, though valid, suffers from a lot of engineering problems: manufacturing issues related to the array, and mechanical shift that requires moving parts in the setup. However, the main problem is that it requires direct contact with the inspected object, which is not possible in many imaging scenarios.

In this Letter, we propose projecting the Barker-based array onto the inspected object using a phase-only spatial-light modulator (SLM). The projection of the array solves all the abovementioned problems, as all the mask manufacturing, mechanical shifting, and interaction with the object are done digitally.

The design of the phase image that is uploaded to the SLM involves an iterative process that relies on the revised Gerchberg-Saxton (GS) algorithm [12,13]. The Barker-based array needs to be created on an object that is placed at a certain distance from the SLM. Therefore, the design is for a SLM phase that after certain free-space propagation (FSP) will transform into the desired Barker-based array. The GS process is performed by the following method (as schematically illustrated in Fig. 3).

The amplitude A_1 is defined to be the Barker-based array, and a zero phase ϕ_1 is imposed in order to define the output plane E_1 . This field then undergoes FSP a distance of $-dz$ to define the input plane E_0 . Since the SLM is phase only, the amplitude of E_0 is imposed to be a constant value (of ones), while the phase ϕ_0 is being kept. The field E_0 undergoes FSP a distance of $+dz$ to the output plane E_1 . This process is then repeated numerous iterations. In every iteration, the amplitude of E_1 , obtained by the FSP, is compared to the Barker amplitude. When the correlation coefficient between the two is higher than a predetermined value, the phase retrieval

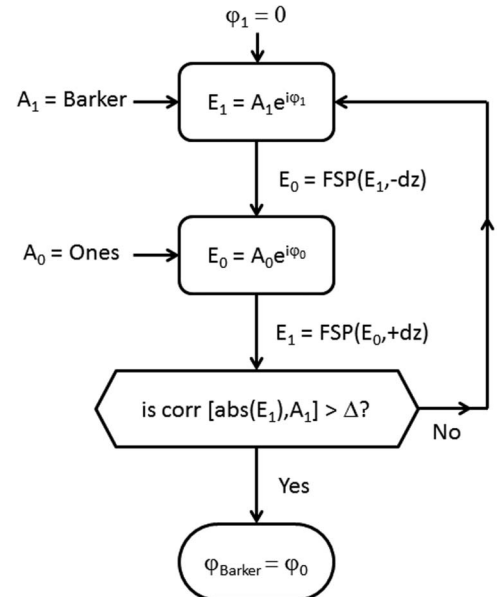


Fig. 3. Iteration flowchart of the GS process.

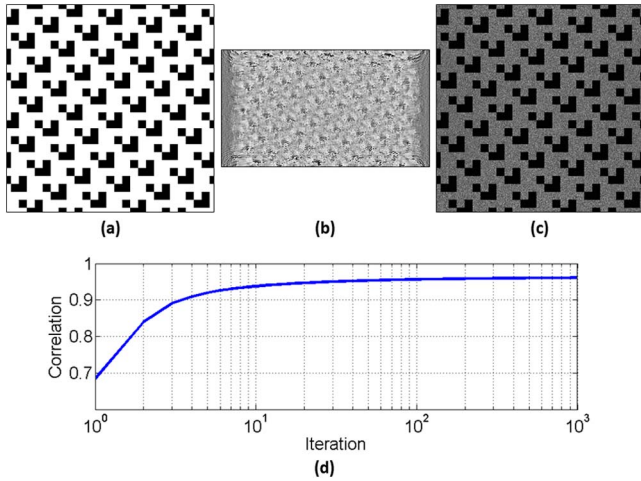


Fig. 4. Phase design using the revised GS process. (a) Desired Barker-based array. (b) The phase result that is uploaded to the SLM. (c) The amplitude results after FSP of $dz = 0.55$ m. (d) The correlation coefficient between (a) and (c) during the GS process.

of the input plane is achieved. Since the GS process is performed independently from the imaging process, the time required for generating the phase masks is not significant (in our case it was a few hours).

The results of the phase design using the revised GS process for $dz = 0.55$ m are presented in Fig. 4. This distance was chosen so that the SLM duplications in the later experiment will not overlap. Figure 4(a) is the desired Barker-based array, Fig. 4(b) is the phase-only GS result that is uploaded to the SLM, and Fig. 4(c) is the obtained amplitude results after FSP of the phase mask for the distance of dz . Figure 4(d) presents the correlation coefficient between the desired Barker-based amplitude image [Fig. 4(a)] and the FSP result [Fig. 4(c)], in a semi-log scale. The correlation converges to 0.96.

The proposed method was tested using the experimental setup presented in Fig. 5. The setup is divided into two main parts: projection and imaging. The projection part consists of a green laser beam at a wavelength of 532 nm (Photop DPGL-2100F), a $\times 3$ beam expander (Newport T81-3X), and a $\times 10$ beam expander (Thorlabs BE10M-A). The total $\times 30$ expansion of the laser beam is

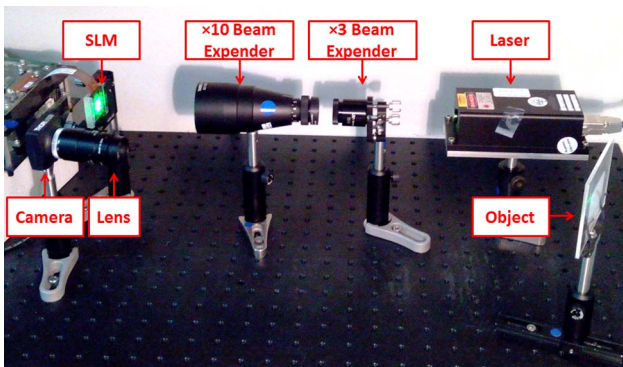


Fig. 5. Experimental setup. A green laser, expanded $\times 3$, and then $\times 10$, illuminating the SLM and reflected onto the object. The object is then imaged by a lens and a camera.

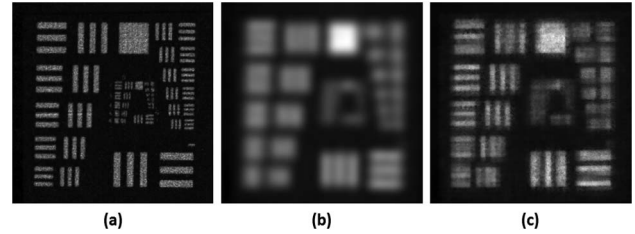


Fig. 6. SR experimental results. (a) HR object. (b) LR image. (c) SR image using the proposed method.

required in order to achieve an almost uniform illumination of the SLM. The SLM is a phase-only reflective liquid-crystal-on-silicon micro display with 1920×1080 pixels resolution and pixel's pitch of $8 \mu\text{m}$ (Holoeye SLM device HEO 1080P). The object was a USAF target located 550 mm from the SLM. The imaging part consists of a 50 mm imaging lens (Navitar MVL50M23), located 500 mm from the object, and a USB camera (Thorlabs DCC1545M).

13 different phase masks were displayed using the SLM. Each phase mask generates a shifted Barker-based array at the object plane. 13 low-resolution (LR) images were captured, each one corresponding to a specific position of the array. The LR images in the experiment had resolution about 20 times smaller than HR reference images. The Barker-based array feature size at the object plane was ~ 0.4 mm, which translates to ~ 8.5 pixels in the camera.

The SR results, obtained using the proposed technique, are presented in Fig. 6. Figure 6(a) is the HR reference image, Fig. 6(b) is the LR image, and Fig. 6(c) is the SR image, achieved using the projected Barker-based array and the mismatched filter. The resolution improvement is clearly visible.

To conclude, using the 2D Barker-based array as the encoding mask for the conventional TMSR method is a very promising concept. The use of a mismatched array with perfect CC properties allows SR imaging with only a small number of images. Projecting the array, instead of placing it directly on the object, offers a much more flexible imaging system that can be suitable to more complex scenarios where accessing the object is not feasible. The phase-calculation process using the revised GS algorithm and a laboratory experiment demonstrating the proposed concept were presented. The SLM has a 60 Hz frame rate. Thus, using proper software, the whole SR imaging process (that requires only 13 images) may take less than 0.25 s.

References

1. R. Otto and L. Fritz, *Die lehre von der bildentstehung im mikroskop von Ernst Abbe* (Vieweg Braunschweig, 1910).
2. M. Françon, *Nouvo Climento Suppl.* **9**, 283 (1952).
3. W. Lukosz, *J. Opt. Soc. Am.* **56**, 1463 (1966).
4. A. Shemer, D. Mendlovic, Z. Zalevsky, J. Garcia, and P. G. Martinez, *Appl. Opt.* **38**, 7245 (1999).
5. A. Ilovitsh, E. Preter, N. Levanon, and Z. Zalevsky, *Opt. Lett.* **40**, 163 (2015).
6. R. H. Barker, *Commun. Theory*, 273–287 (1953).
7. N. Levanon and E. Mozeson, *Radar Signals* (Wiley, 2004).

8. J. García, Z. Zalevsky, and D. Fixler, *Opt. Express* **13**, 6073 (2005).
9. S. Alquaddoomi and R. A. Scholtz, *IEEE Trans. Inf. Theory* **35**, 1048 (1989).
10. J. A. Davis, J. Jedwab, and K. W. Smith, *Proc. Am. Math. Soc.* **135**, 2011 (2007).
11. R. Turyn and J. Storer, *Proc. Am. Math. Soc.* **12**, 394 (1961).
12. W. R. Gerchberg and W. O. Saxton, *Optik (Stuttg.)* **35**, 237 (1972).
13. E. Gur and Z. Zalevsky, *J. Electron. Imaging* **18**, 033016 (2009).